

## Observation of a Relaxed Plasma State in a Quasi-Infinite Cylinder

T. Gray,\* M. R. Brown, and D. Dandurand

*Department of Physics and Astronomy, Swarthmore College, Swarthmore, Pennsylvania 19081-1397, USA*

(Received 15 November 2012; published 22 February 2013)

A helical relaxed plasma state is observed in a long cylindrical volume. The cylinder is long enough so that the predicted minimum energy state is a close approximation to the infinite cylinder solution. The plasma is injected at  $v \geq 50$  km/s by a coaxial magnetized plasma gun located at one end of the cylindrical volume. The relaxed state is rapidly attained in 1–2 axial Alfvén times after initiation of the plasma. Magnetic data are favorably compared with an analytical model. Magnetic data exhibit broadband fluctuations of the measured axial modes during the formation period. The broadband activity rapidly decays as the energy condenses into the lowest energy mode, which is in agreement with the minimum energy eigenstate of  $\nabla \times \mathbf{B} = \lambda \mathbf{B}$ .

DOI: [10.1103/PhysRevLett.110.085002](https://doi.org/10.1103/PhysRevLett.110.085002)

PACS numbers: 52.25.Xz, 52.30.Cv, 52.55.Ip

The magnetic field structure of plasmas that has undergone relaxation with the magnetic helicity ( $H_b$ ) as an invariant can be described by the force free equation,

$$\nabla \times \mathbf{B} = \lambda \mathbf{B}, \quad (1)$$

where  $\lambda$  is a constant. The magnetic helicity is expressed as

$$H_b \equiv \int \mathbf{A} \cdot \mathbf{B} dV, \quad (2)$$

where  $\mathbf{A}$  is the magnetic vector potential. The system, absent of flows, minimizes the total magnetic energy, constrained by the total magnetic helicity, and relaxes to its minimum energy state. This process is known as Woltjer-Taylor relaxation [1,2]. Woltjer showed that force-free states with constant  $\lambda$  [i.e., solutions to Eq. (1)] are the lowest energy states for a closed system [2]. Given an appropriate dissipation mechanism, the magnetic energy could selectively decay faster than the magnetic helicity, providing a means for a magnetic system to relax to this preferred final state of minimum energy. Taylor stated that given a finite resistivity, magnetic reconnection approximately conserves the global helicity and provides for the dissipation mechanism for reducing the magnetic energy [1,3]. The selective decay hypothesis posits that the energy selectively decays relative to the magnetic helicity because the energy spectra peaks at higher wave numbers, where dissipation is higher [4,5].

In the laboratory, experiments which rely on plasma relaxation are often confined with the help of flux conserving boundaries. In singly connected volumes, the final structure of the minimum energy state is determined purely by the geometry of the flux conservers. In cylindrical geometries, the symmetry about the  $z$  axis, denoted by the azimuthal mode number  $m$ , of this minimum energy state is determined by the aspect ratio of the cylinder. The critical aspect ratio is  $L/a = 1.67$ , where  $L$  and  $a$  are the length and radius of the cylinder [6,7]. Plasmas with aspect ratios lower than this critical number are axisymmetric

( $m = 0$ ) and are called spheromaks [8]. Above this critical aspect ratio, plasmas are nonaxisymmetric ( $m = 1$ ) in nature, and as the aspect ratio increases, tend towards a universal double helix state, the Taylor double helix [3,9].

In the case of an infinite cylinder, the minimum energy state corresponds to the  $\lambda a = 3.11$  solution. This double helix state has a helical pitch of  $ka = 1.234$ , where  $k$  is the wave number associated with the  $z$  axis. In the case of a cylinder of finite length, the value of  $\lambda a$  increases as the aspect ratio decreases.

It should be noted that the Taylor double helix state was introduced in the context of the toroidal geometry found in the reversed field pinch (RFP). As RFPs always have some amount of toroidal (axial) flux, the double helix state as initially proposed also has this toroidal flux component. Given this toroidal flux component, there are two possible sets of solutions to Eq. (1). The first is a purely “symmetric” mode ( $m = 0, k = 0$ ), representing only the toroidal flux, while the second is a “mixed” solution, combining the symmetric solution and other terms. In the case of the mixed solution, the minimum energy state selected is again the one that minimizes  $\lambda$  [3]. This smallest root occurs for  $m = 1, ka \approx 1.25$ , and is given by  $\lambda a = 3.11$  [3].

Whether or not the symmetric or mixed solution is selected is determined by the value of the pinch parameter,  $\theta = \frac{2I}{aB_0}$ , where  $I$  is the plasma current responsible for generating the poloidal fields, and  $B_0$  is the toroidal field. When the pinch parameter exceeds a certain value,  $\theta \sim 1.6$ , the mixed solution is the minimum energy state of the plasma. This is notable because this solution has the same  $\lambda a$  and  $ka$  values as the minimum energy state of an infinite cylinder, though the latter does not have the symmetric solution mixed in, which is necessary to represent the toroidal flux of RFPs. Thus, the infinite cylinder solution is analogous to the minimum energy state solution to Eq. (1) found in RFPs where the pinch parameter equals the critical value of  $\theta \sim 1.6$ . Quasi-single-helicity states, in which there is a single  $m = 1$  mode which dominates other

existing modes, have been observed in RFPs [10]. However, these Quasi-single-helicity states are not the same as the Taylor double helix and do not have  $ka = 1.25$ .

The Swarthmore Spheromak Experiment (SSX) [11] has recently been performing experiments in a plasma “wind tunnel” configuration. In this configuration, a coaxial magnetized plasma gun is mounted on one end of and blows plasma into a long cylindrical copper flux conserver, 104 cm long and 7.8 cm in radius, giving it an aspect ratio of  $L/a = 13.4$ . A cross section of the SSX is shown in Fig. 1(a). The plasma gun fields and vacuum fields in the flux conserver are nearly axisymmetric. The flux conserver that the gun injects plasma into is fully evacuated; there is no fill gas or target plasma. The plasma is axisymmetric as it first emerges from the gun, consistent with an axisymmetric spheromak. However, it rapidly undergoes an instability and becomes nonaxisymmetric. An observation of relaxation to a nonaxisymmetric plasma state has previously been made in the SSX device, albeit with the much smaller aspect ratio of  $L/a = 3.0$  [12].

The  $\lambda a$  for the minimum energy state for the wind tunnel flux conserver was calculated using a method similar to the one outlined by Finn *et al.* [7], modified to utilize singular value decomposition. This resulted in  $\lambda a = 3.136$ , which is within 1% of the  $\lambda a$  value of 3.11 for the infinite cylinder state. As such, the wind tunnel flux conserver has dimensions sufficient to provide for a minimum energy state that is a close approximation of the infinite cylinder solution, ignoring the very ends of the geometry. Also of note is the

closeness of the values of the helical pitch  $ka$  for the wind tunnel and the infinite cylinder case. The wind tunnel’s minimum energy state possesses  $ka = 1.292$ , which is within 5% of the infinite cylinder’s  $ka = 1.234$ . The magnetic configuration for this minimum energy state can be generated using the procedure outlined by Morse [13] and can be seen in Fig. 1(b).

In order to experimentally measure the helical pitch of the wind tunnel plasma, a long axial magnetic probe was installed along the  $z$  axis of the flux conserver. The probe was constructed to measure the magnetic field in two orthogonal directions, perpendicular to the  $z$  axis. The data from the probe were hardware integrated and digitized at 10 MHz. This measured magnetic field is plotted in Fig. 2 alongside of the calculated  $B$  field [from Fig. 1(b)], taken along the  $z$  axis. Strong agreement between the measured and calculated  $B$  fields on the axis is evident. The experimental data in Fig. 2 are from a single plasma discharge at  $48 \mu\text{s}$ , well after the plasma has settled into a relaxed state (see Fig. 3).

Utilizing the magnetic probe’s 19 positions, the data can be spectrally analyzed to determine the activity at different values of  $ka$  as a function of time. During the formation and relaxation phase between 25–35  $\mu\text{s}$ , the plasma exhibits lots of activity at all of the  $ka$  modes the probe is capable of sensing. Very quickly [ $\mathcal{O}(\tau_A)$ ], the activity at the higher values of  $ka$  dissipates as the energy accumulates in the lowest  $ka$  mode supported by the geometry of the flux conserver. This is consistent with the process of selective decay. It should be noted that the spacing of the coil locations on the probe used to generate Fig. 3 is 4.8 cm. This limits  $ka$  ‘bins’ in Fig. 3 to discrete quantities, separated by  $\sim 0.533$ . The predicted value  $ka = 1.292$  straddles the two nearest bins in the plot,  $ka = 1.066$  and  $ka = 1.599$ .

In order for the plasma to be fully relaxed into a Woltjer-Taylor state, the value of  $\lambda$  must be spatially uniform. Radial magnetic probes installed for the purpose did not measure flat  $\lambda$  profiles (not shown) [14]. There are several

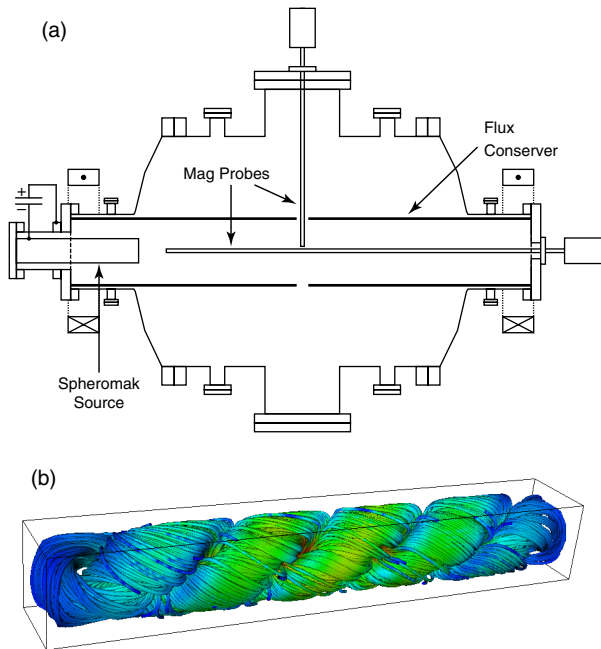


FIG. 1 (color online). (a) A schematic of the SSX vacuum vessel is shown. (b) The streamlines of the magnetic field in the calculated lowest energy state according to the Taylor theory is shown, with color representing the relative magnitude of  $|B|$ .

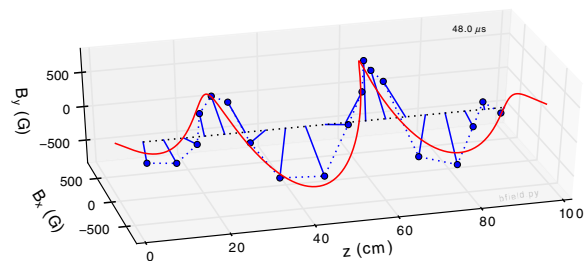


FIG. 2 (color online). A comparison of the axial magnetic field of the calculated lowest energy state and the measured axial magnetic field in the relaxed plasma. The calculated field is the solid (red) line while the measured fields are illustrated by vectors (blue) extending from the  $z$  axis. The heads of the vectors are connected by a dotted (blue) line for clarity. Both the calculated and measured axial fields are consistent with an  $m = 1$  plasma.

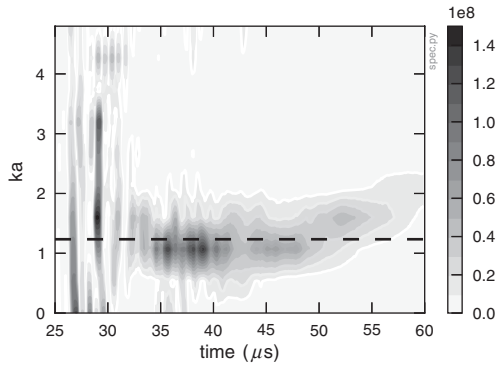


FIG. 3. Decay of the higher  $ka$  modes to the lowest energy mode. The lowest energy mode should have  $ka = 1.292$ , marked with the dashed line.

possible explanations for the lack of a flat  $\lambda$  profile. Taylor relaxation assumes a low- $\beta$  plasma, where the only significant source of free energy is in the magnetic fields. Measurements of the plasma  $\beta$  in the SSX result in  $\beta \sim 40\%$  for most of the lifetime of the plasma, as seen in Fig. 4. During this period of stable  $\beta$ ,  $B^2$  drops rapidly, which is balanced by a corresponding drop in  $T_i$  and, to a smaller degree, a drop in  $n_e$ .  $\beta$ 's this high may prevent the plasma from reaching a final state completely dictated by the Taylor relaxation theory. The plasma  $\beta$  is measured by using the mean  $\mathbf{B}$  measured along the radial magnetic probe in conjunction with line averaged measurements of  $T_e$ ,  $T_i$ , and  $n_e$ .

In addition to the high  $\beta$ , the plasma also exhibits large flows, axially and azimuthally, both during the formation phase and after the plasma has relaxed into a final state [15]. Flow velocities on the order of the ion sound speed were consistently measured during the lifetime of the plasma. Like the high  $\beta$ , large flow velocities are not provided for under the Taylor relaxation theory and could contribute to relaxation to a state that does not fully comply with the theory.

Despite this, the double helix structure with a specific helical pitch is robust in the face of nonzero plasma pressure and high velocity flows. It is possible that the initial cross helicity ( $H_c$ ) content

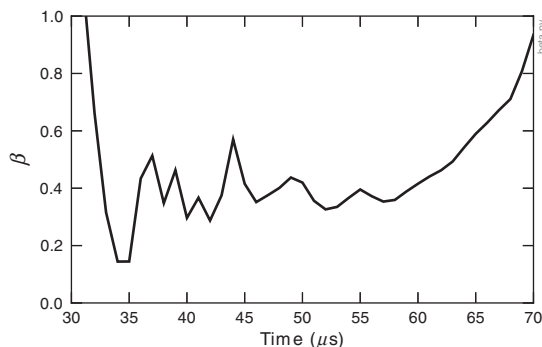


FIG. 4. Plasma  $\beta$  calculations show  $\beta \sim 40\%$  for most of the plasma lifetime.

$$H_c = \int \mathbf{v} \cdot \mathbf{B} dV \quad (3)$$

is high enough that the dynamic alignment relaxation process, where  $\mathbf{v}$  and  $\mathbf{B}$  become aligned, partially influences the plasma relaxation [16,17].

Though dynamic alignment is mostly observed in systems with little magnetic helicity, it is feasible to have systems where both selective decay and dynamic alignment govern the relaxation process [18]. The initial balance between  $H_b$  and  $H_c$  dictates the nature of the final minimum energy state. A system where  $H_b$  is relatively more important should relax to a state that is more similar to a Taylor state, in accordance with selective decay being the dominating contributor to the relaxation process. One where  $H_c$  is more significant shares more in common with pure dynamic alignment states. This initial balance also determines the ratio of kinetic and magnetic energy in the final state. The relatively high  $\beta$  observed in this system points to the possibility of such an interplay between relaxation processes. In light of this, it is notable that the helical pitch of the final plasma state is in such good agreement with the predicted Taylor state, even though selective decay may not be the only relaxation process contributing.

Another notable characteristic of this state is the rapidity of the relaxation process. Global relaxation to the Taylor state should occur over many eddy turnover times. In the system described here, the radial Alfvén transit time ( $\tau_A$ ) for the system is  $\sim 1-2 \mu s$ . Looking at the  $ka$  spectrum in Fig. 3, it is clear that the transition from an unorganized plasma to a structure with a close approximation of the Taylor state's helical pitch ( $k = 1.292$ ) is very abrupt and takes  $\mathcal{O}(\tau_A)$ . Servidio *et al.* [19] detail simulations which observe the rapid and simultaneous magnetohydrodynamic relaxation into localized patches of plasma with near alignment of  $\mathbf{J}$  and  $\mathbf{B}$ . These patches of locally relaxed plasma can then negotiate with adjacent patches to reach a globally relaxed state on a longer time scale, but many of the characteristics of relaxation will be evident locally. This localized relaxation might explain the rapidity of the transition observed in the double-helix plasmas as well as the lack of a flat radial  $\lambda$  profile. The volumes sampled by the radial probes might be approximately force free, but other regions of locally relaxed plasma might exist elsewhere that are not sampled. Occasionally, activity not consistent with the self-similar decay expected in a fully relaxed state is observed late in time on the radial magnetic probe, supporting the idea that the double helix structure of the plasma emerges rapidly, even when the plasma is only partially relaxed.

Unfortunately, the lifetime of the SSX plasma is short enough ( $40 \mu s$ ) that it might not have time to fully relax before collapsing. Interactions with the plasma facing surfaces are expected to be high given the relatively small radius of the wall (8 cm) compared to the potential range of

ion gyroradii (0.5–2 cm). Large levels of plasma-wall interactions can degrade plasma confinement, leading to a shorter lifetime. Baking and glow-discharge cleaning are used to help partially mitigate this problem.

In summary, we present the observation of plasma relaxation in a “quasi-infinite” cylinder, i.e., a cylindrical geometry sufficiently long to approximate an infinite cylinder with respect to its minimum energy state. The relaxed state possesses the same helical pitch of the Taylor double helix, despite high velocity flows and a high plasma  $\beta$ . These factors might contribute to the lack of full agreement with the minimum energy Taylor state, which can possibly be explained by generalized relaxation processes or fast, patchy relaxation.

This work was supported by the Department of Energy and the National Science Foundation. We would like to thank John Finn for valuable discussions on the series solutions for relaxed states in cylinders of arbitrary length, Slava Lukin for general discussions, and Steve Palmer and Jim Haldeman for their technical support.

---

\*tgray1@gmail.com

- [1] J. B. Taylor, *Phys. Rev. Lett.* **33**, 1139 (1974).
- [2] L. Woltjer, *Proc. Natl. Acad. Sci. U.S.A.* **44**, 489 (1958).
- [3] J. B. Taylor, *Rev. Mod. Phys.* **58**, 741 (1986).

- [4] W. H. Matthaeus and D. Montgomery, *Ann. N.Y. Acad. Sci.* **357**, 203 (1980).
- [5] D. Montgomery, L. Turner, and G. Vahala, *Phys. Fluids* **21**, 757 (1978).
- [6] A. Bondeson, G. Marklin, Z. G. An, H. H. Chen, Y. C. Lee, and C. S. Liu, *Phys. Fluids* **24**, 1682 (1981).
- [7] J. M. Finn, W. M. Manheimer, and E. Ott, *Phys. Fluids* **24**, 1336 (1981).
- [8] T. R. Jarboe, *Plasma Phys. Controlled Fusion* **36**, 945 (1994).
- [9] M. J. Schaffer, *Phys. Fluids* **30**, 160 (1987).
- [10] D. F. Escande, P. Martin, S. Ortolani, A. Buffa, P. Franz, L. Marrelli, E. Martines, G. Spizzo, S. Cappello, A. Murari, R. Pasqualotto, and P. Zanca, *Phys. Rev. Lett.* **85**, 1662 (2000).
- [11] M. R. Brown, *Phys. Plasmas* **6**, 1717 (1999).
- [12] C. D. Cothran, M. R. Brown, T. Gray, M. J. Schaffer, and G. Marklin, *Phys. Rev. Lett.* **103**, 215002 (2009).
- [13] E. C. Morse, *J. Math. Phys. (N.Y.)* **46**, 113511 (2005).
- [14] The axial and radial probes could not be used simultaneously.
- [15] X. Zhang, D. Dandurand, T. Gray, M. R. Brown, and V. S. Lukin, *Rev. Sci. Instrum.* **82**, 033510 (2011).
- [16] M. Dobrowolny, A. Mangeney, and P. Veltri, *Phys. Rev. Lett.* **45**, 144 (1980).
- [17] W. H. Matthaeus, M. L. Goldstein, and D. C. Montgomery, *Phys. Rev. Lett.* **51**, 1484 (1983).
- [18] T. Stribling and W. H. Matthaeus, *Phys. Fluids B* **3**, 1848 (1991).
- [19] S. Servidio, W. H. Matthaeus, and P. Dmitruk, *Phys. Rev. Lett.* **100**, 095005 (2008).